ISA
TRANSACTIONS®

ISA Transactions 43 (2004) 205–216

Friction identification in mechatronic systems

Bashir M. Y. Nouri*

Department of Mechatronics Engineering, Faculty of Engineering, The Hashemite University, P. O. Box 150459, Zarqa 13115, Jordan

(Received 4 December 2002; accepted 2 August 2003)

Abstract

Since no universal friction model exists and the practical measurement of friction is not straightforward, this paper presents an experimental method of identifying friction in mechatronic systems. Friction is perhaps the most important nonlinearity that is found in any mechatronic system of moving parts and influences the system in all regimes of operation. For the purpose of improving the performance of mechatronic systems and solving their servo problem, a better understanding of friction behavior in its two basic regimes is needed. In this paper, the two basic friction regimes, viz., presliding with its hysteresis behavior, which is predominantly position dependent, and gross sliding, which is predominantly velocity dependent, are well exposed and identified. © 2004 ISA—The Instrumentation, Systems, and Automation Society.

Keywords: Friction; Identification; Experimental; Mechatronic systems

1. Introduction

Friction is perhaps the most important nonlinearity that is found in any mechatronic system with moving parts. Experimental identification of friction in mechatronic systems will be demonstrated by using a pneumatic servo positioning system. For the considered pneumatic servo positioning system, friction, which arises in the contacts of the piston with the cylinder walls as well as in the linear slideway and other minor rubbing elements has a direct impact on the system in all regimes of operation. In order to design accurate compensation, friction has to be experimentally identified and modeled. This task is by no means a simple one since no universal friction model exists, and on the other hand, the practical measurement of friction is not straightforward.

This paper deals with experimental friction identification in the two basic regimes: pre-sliding friction, which is predominantly position dependent (function of pre-sliding displacement), and gross sliding friction, which is predominantly velocity dependent (function of sliding velocity). Section 2 presents the test setup that is used for the experimental identification of friction in mechatronic systems. Section 3 presents the nature of pre-sliding friction, showing that the asperity junctions of the contacting surfaces behave as nonlinear springs prior to breaking. This lies at the basis of pre-sliding hysteresis friction, explaining why it is displacement dependent. This section also identifies the *nonlocal* memory character of pre-sliding hysteresis friction. Section 4 presents the experimental identification of the breakaway (or static) friction force. Section 5 identifies the gross sliding friction force and showing the hysteretic behavior of friction in the velocity or what is termed ''frictional lag'' (with respect to velocity change). Sec-

E-mail address: bashir_nouri@yahoo.com

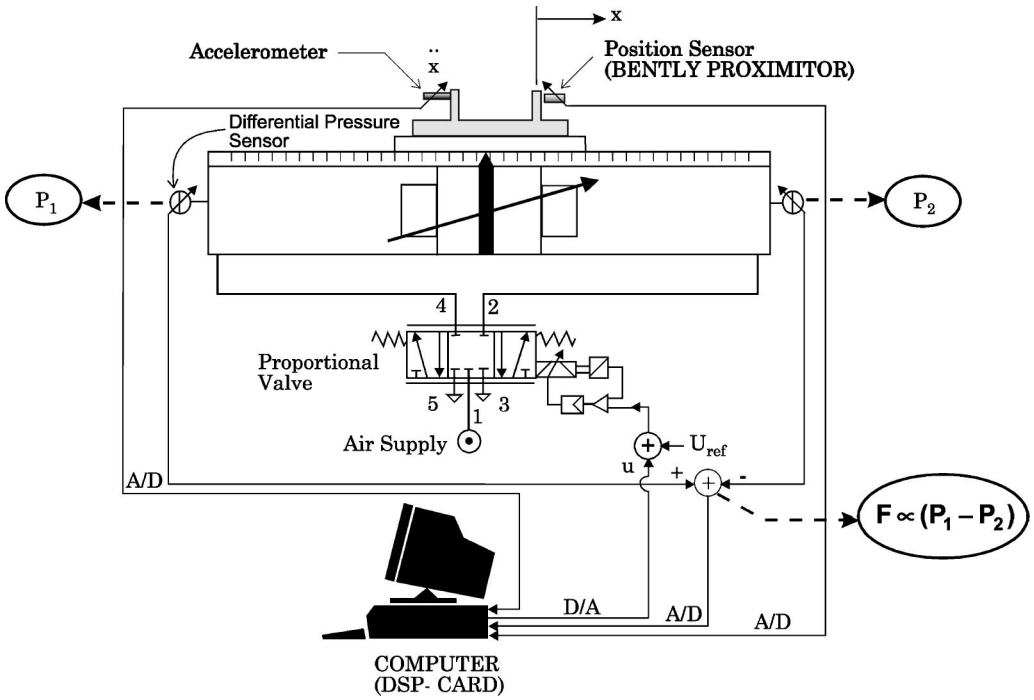

Fig. 1. Friction identification test setup.

tion 6 concludes the paper with some comments and statements.

2. Friction identification test setup

A schematic representation of the test setup configuration used for the demonstration of our experimental method of identifying friction in mechatronic systems is shown in Fig. 1. The considered mechatronic system is a pneumatic servo positioning system. The test setup consists of a 5/3-way proportional directional control valve and a rod less pneumatic cylinder. The two pressure sensors are used for measuring the pressure difference between the chambers of the cylinder; which is proportional to the driving force. The position sensor, a noncontacting eddy current sensor with a range of about 2 mm, is used for measuring the pre-sliding displacement. (The cylinder is equipped with an integrated ultrasonic position sensor that is, however, not used in these experiments owing to its limited resolution, 50 μm.) The acceleration is measured by a carrier signal, inductive accelerometer, with frequency range of 0–250 Hz. The noise in the measured signals is filtered by analog resister-inductor-capacitor (RLC) filters with 1.2-KHz cutoff frequency, while the maximum used sampling frequency is 1 KHz. The velocity is obtained by integrating the measured acceleration. The computer is equipped with a digital signal processor (DSP-card) that is used for sending a driving signal to the proportional valve via a D/A converter and reading all the sensors via A/D converters.

Our procedure for measuring friction is by measuring acceleration and subtracting computed inertial forces from the measured applied forces that are deduced from the measured pressure difference in the chambers of the cylinder.

3. Pre-sliding friction identification

The aim here is to measure the friction force in function of the displacement, prior to gross sliding, and to verify the spring and hysteretic behavior of the asperity junctions of the contacting surfaces.

3.1. Spring behavior of the asperity junctions

The spring behavior of the asperity junctions of the contacting surfaces can be verified by experiments. The procedure here is to ramp up the ap-

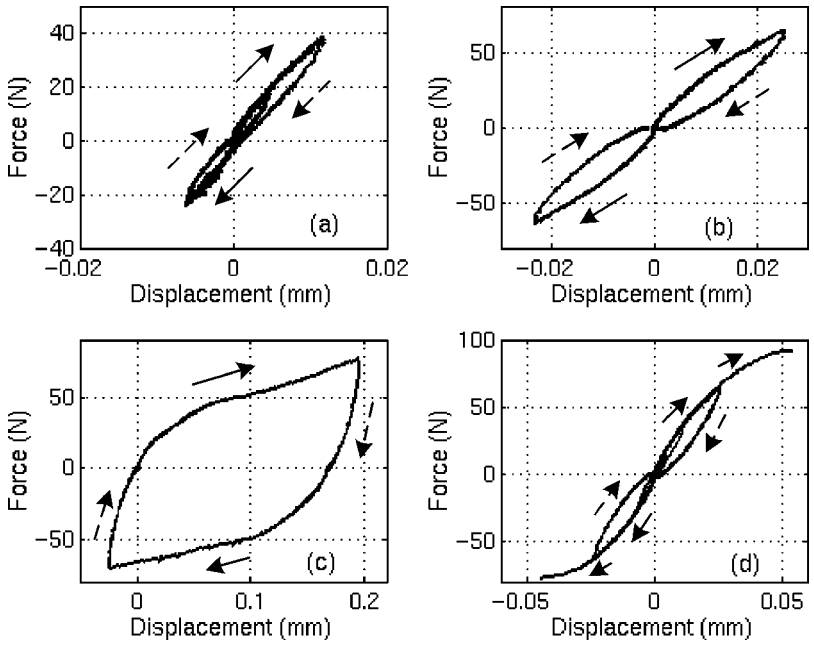

Fig. 2. Nonlinear spring behavior of the asperity junctions.

plied force to a level below the breakaway friction force (see later) and suddenly remove the applied force, i.e., set the applied force equal zero and wait for some time. During this process, the asperity junctions will deform elastically and/ or plastically (depending on the level of the ramped up applied force). When the force is set equal zero, the elastic deformation of the asperity junctions will disappear and the sliding part of the mechatronic system will be at a distance equal to the plastic deformation of the asperity junctions from its original location (the used reference location of the slider). During these experiments, you have to record the friction force and the displacement of the slider.

The spring behavior of the asperity junctions of the contacting surfaces in the considered pneumatic actuator is verified by experiments. Several experiments have been performed on the test setup, Fig. 1, for identifying the spring behavior of the asperity junctions. Using the previous experimental procedure, all the results proved that the asperity junctions in the system exhibit a nonlinear spring behavior as described here below:

1. If a small positive or negative force is ramped up, an elastic deformation of the asperities will occur. If the applied force is removed, the stored energy in the asperity junctions is partially recovered and the deformation disappears, i.e., the slider returns back to its original location after the applied force has been removed; see Fig. 2(a).
2. Plastic deformation takes place after a certain value of elastic deformation. If a force is ramped up to a value higher than that in part 1 and then removed, the elastic deformation will disappear and the slider will be at a new location at a distance equivalent to the plastic deformation of the asperity junctions from its original location; see Fig. 2(b).
3. If a force is ramped up to a value smaller than the breakaway friction in a given direction (e.g., the positive direction), then removed, and the same force is ramped up again in the opposite direction, then removed, the operation results in a kind of hysteresis loop, see Fig. 2(c), where the total elastic and plastic deformation of the asperity junctions can be found, also the total dissipated energy (work) and the recovered energy from the elastic deformation can be calculated from the hysteresis loop.

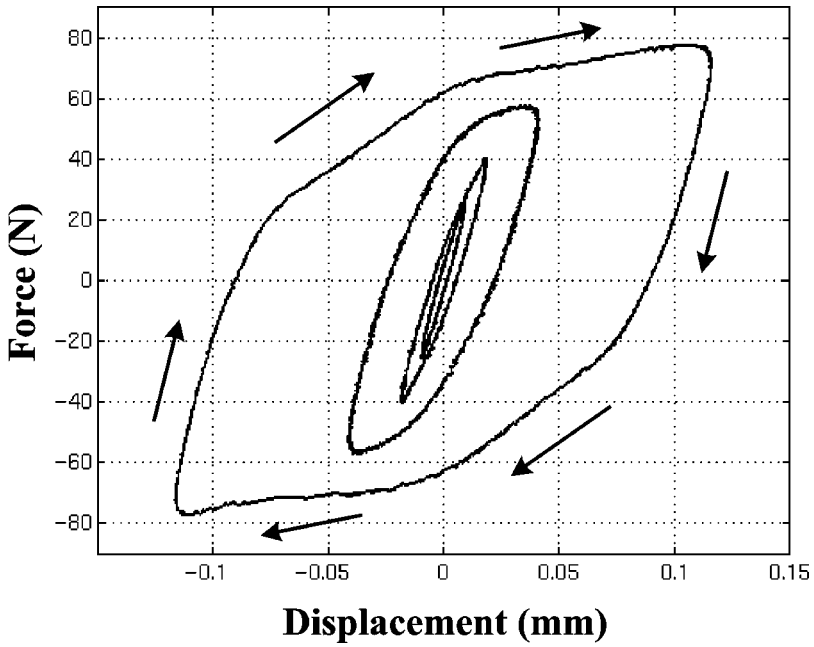

Fig. 3. Hysteresis loops for different range of pre-sliding displacement. The largest loop corresponds to cylinder pressure variation with respect to supply pressure of 7-bar level, and the smaller loops correspond to cylinder pressure variations with respect to supply pressure of 2-bar level.

4. If a force is ramped up to a value greater or equal to the level of static friction, the asperity junctions will break and a true sliding occurs, see Fig. 2(d).

3.2. Hysteresis behavior of pre-sliding friction

The aim here is to measure the friction force in function of the displacement, prior to gross sliding, and to verify its hysteretic behavior. The hysteresis behavior of the asperity junctions proves that pre-sliding friction dissipates energy. Hysteresis behavior, as a natural phenomenon which exists not only in pre-sliding friction but also in other systems such as magnetism, consists of branches and extrema. A branch of hysteresis friction is the path representing the behavior of the friction phenomenon between two extrema. The two extrema are the maximum and minimum force of the hysteresis friction loop or the two reversal points where the system changes its direction.

The shape and the size of the hysteresis loop depend among other things on the material of the contacting surfaces [1]. This result leads us to take into account some mechanical considerations in studying the hysteresis behavior in the considered mechatronic system (the pneumatic actuator) such as the metal-rubber contact and the cylinder pressure variations. Tutuko Prajogo [2] and Futami [3] proved experimentally that the frequency of the excitation signal does not have any influence either on the shape or on the size of a hysteresis loop for a wide frequency range.

The hysteresis loops depend on the pre-sliding displacement only. Fig. 3 shows small and large hysteresis loops for different range of pre-sliding displacement and cylinder pressure variations that are obtained experimentally using the experimental setup of Fig. 1. Sinusoidal excitation signals are used and different cylinder pressure variations are applied. The results show that the cylinder pressure variations do not have an influence on the shape of the hysteresis loop but do have an influence on the size of the hysteresis loop, i.e., the two extreme (the minimum and maximum force of the hysteresis loop, see Section 4) are function of cylinder pressure variations corresponding to supply pressure. The results are also show that the hysteresis friction behavior in the pneumatic actuator depends on the pre-sliding displacement. The metal-rubber contact leads to a large pre-sliding

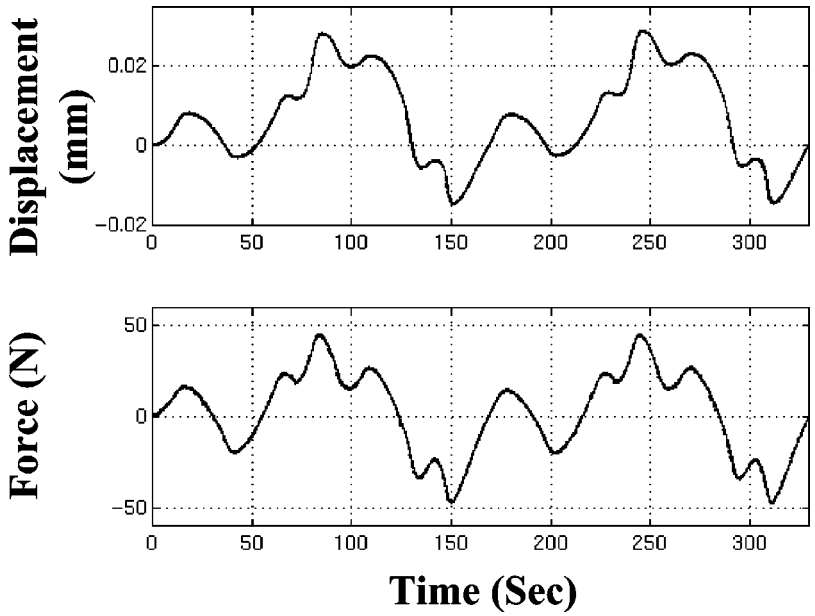

Fig. 4. Measured pre-sliding displacement and force.

displacement, i.e., the pre-sliding displacement in metal-rubber contact is much larger than that in metal-metal contact.

There are two main types of hysteretic behavior. First, hysteresis with *nonlocal* memory means that the future values of the function (friction force in this case) at some instant of time t ($t \geqslant t_o$) depend not only on its present value at the instant of time t_o and the value of its argument (displacement in this case) but also on the past extremum values of the function. This property is in contrast to the behavior of hysteresis nonlinearities with *local* memory, where the past has its influence upon the future through the current value of the function [4]. The *nonlocal* memory character of pre-sliding hysteresis friction, in the pneumatic actuator, has been thoroughly verified by test. For this purpose, a periodic piston motion trajectory is chosen with several velocity reversal points (per period), within the pre-sliding region, an example of such a trajectory is shown in Fig. 4 together with the pre-sliding force. When the two sets of measured synchronized data are plotted against each other, an external loop is obtained with several internal loops within it, see Fig. 5(d). Fig. 5 shows examples of measured hysteresis friction with *nonlocal* memory in the pneumatic actuator.

3.3. Modeling the pre-sliding friction

Fig. 3 shows typical hysteresis loop measurement for different range of pre-sliding displacement, and corresponding to cylinder pressure variation with respect to supply pressure of 7-bar level (the largest loop) and 2-bar level (smaller loops). Fig. 6 verifies the point-symmetry of the largest hysteresis loop (see Fig. 3), plotting the inverted lower half and upper half on top of one other, so it is sufficient to model only one part (the upper part) of the hysteresis loop. A suitable model of the hysteresis friction force in any direction would be

$$F_h(z) = F_b + F_d(z), \tag{1}$$

where $F_h(z)$ is the hysteresis friction force, i.e., the part of friction force that exhibits hysteretic behavior, F_b is the hysteresis friction force at velocity reversal, and $F_d(z)$ is a point symmetrical strictly increasing function of the asperities average deflection (z) that models a hysteresis branch and can be obtained by identification as the following.

The hysteresis branch can be approximated by a continuous smooth or piecewise linear function on the interval $0 \leqslant z < z_b$, where z_b is the asperity av-

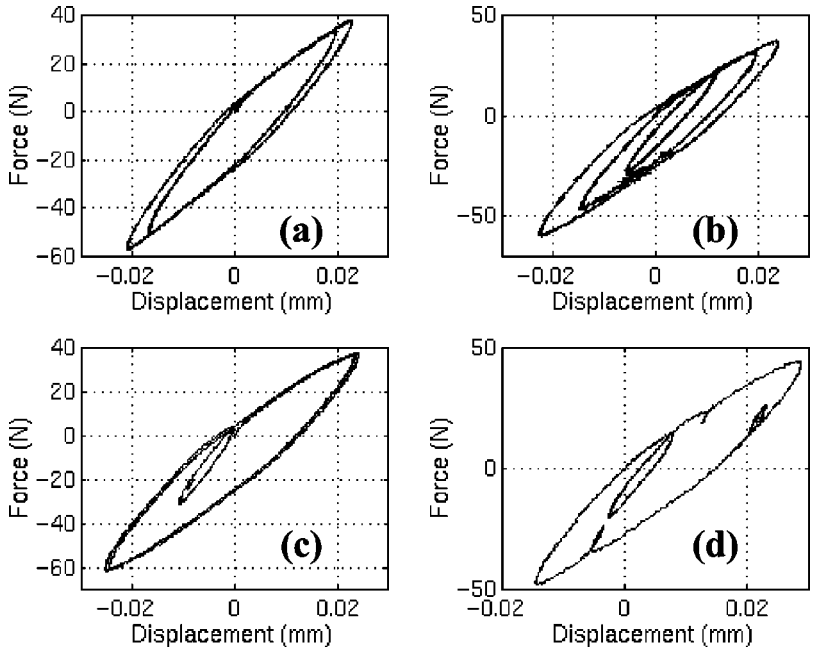

Fig. 5. Measured pre-sliding hysteresis friction behavior with *nonlocal* memory.

erage deflection at the breakaway point of the asperity junctions. Fig. 7 shows a piecewise linear model of the pre-sliding hysteresis branch. The pre-sliding region is divided into three regions depending on the stiffness of the asperity junctions in every region; see Figs. 6 and 7. The model parameters are as follows: k_o is the stiffness of the asperity junctions in the first region, $0 \leqslant z < z_1$, k_1 is the asperity junctions stiffness in the second region, $z_1 \leqslant z < z_2$, k_2 is the asperity junctions stiffness in the third region, $z_2 \leqslant z < z_b$, and the fourth region is the gross sliding region. f_1 and f_2 are the intercepts with the force ordinate (F_d) that can be obtained by a linear fit of the measured pre-sliding displacement and force data in the pre-sliding regions 2 and 3.

Modeling the measured hysteresis branch by a piecewise linear function has the advantage that the physical meaning of the model parameters can

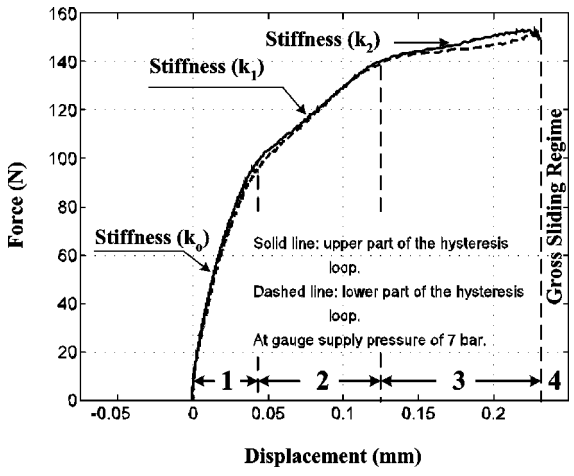

Fig. 6. Point symmetry of the hysteresis loop.

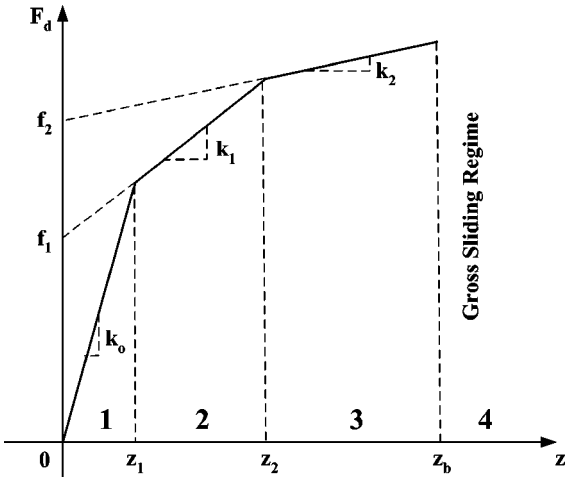

Fig. 7. Piecewise linear model of a pre-sliding hysteresis branch.

be identified in relation with the stiffness of the asperity junctions in the pre-sliding regime, and the same model parameters can then be used directly in a nonlinear model of the hysteresis branch.

Comparing Fig. 6 with Fig. 7, it is clear that in the pre-sliding region 1 and at the start of region 2 the asperity junctions exhibit a nonlinear transition. For this reason, the hysteresis branch will be modeled by a nonlinear (exponential) function in the pre-sliding regions 1 and 2, and with same identified parameters of the piecewise linear model. The point-symmetrical strictly increasing function $F_d(z)$ of the asperities average deflection (z) that models a hysteresis branch and obtained by identification is given by

$$F_d(z)=\begin{cases} k_1 z - f_1(e^{-f_1 z}-1), & 0 \leqslant z < z_2 \\ k_2 z + f_2, & z_2 \leqslant z \leqslant z_b. \end{cases} \quad (2)$$

The implementation of the proposed hysteresis model in programming requires the provision of two memory stacks for the function $F_h(z)$: one for its minimum in ascending order (stack *min*), and one for its maximum (stack *max*). The stacks grow at velocity reversal and shrink when an internal hysteresis loop is closed. When the system goes from pre-sliding to sliding, the stacks are reset and the breakaway (or static) friction force (see Section 4) takes the value of the hysteresis friction force function $F_h(z)$ that will eliminate the discontinuity between the pre-sliding and the gross sliding (see Section 5) friction models. The value of the average deflection of the asperity junctions (z) is reset to zero at each velocity reversal and recalculated at the closing of an internal hysteresis loop. The value F_b [see Eq. (1)] equals the most resent value of stack *max* if the current transition curve is descending and that of stack *min* if the current transition curve is ascending.

The hysteresis friction model is governed by the following mechanisms:

1. Motion reversal: At motion reversal, the function $F_h(z)$ will have a new extreme value, a maximum value of $F_h(z)$ has to be added to stack *max* and a minimum value to stack *min*. Motion reversal initiates a new transition curve by setting F_b equals to the value of $F_h(z)$ at motion reversal, i.e., F_b equals the value of the updated stack. The average deflection of the asperity junctions (z) is reset to zero at every motion reversal.
2. Nonlocal memory: If an internal hysteresis loop is closed between two reversals, it will be removed from the hysteresis memory, and the extreme values that are associated with that loop will be wiped out from the stacks and F_b takes the previous stack value, i.e., the value of the stack before the establishment of that hysteresis loop. The average deflection of the asperity junctions (z) is recalculated from the inverse function of the strictly increasing function $F_d(z)$.
3. Breakaway: At the breakaway point, the average deflection of the asperity junctions (z) is equal to the total traveled displacement before the breakaway (z_b) and $F_h(z)$ is equal to the breakaway (or static) friction force F_S (see Section 4), that will switch on the gross sliding friction model (see Section 5). In this way the discontinuity between the pre-sliding and gross sliding friction models is eliminated.

During gross sliding, z is equal to (z_b) and the involved stack (stack *min* is involved with negative direction and stack *max* is involved with positive direction) tracks the sliding friction force. If stiction occurs, the average deflection of the asperity junction (z) is reset to zero and the involved stack is equal to the most recent sliding friction force. In this way the discontinuity between the gross sliding and the pre-sliding friction models is eliminated. The previous procedure (algorithm) is used for simulating the pre-sliding friction with *nonlocal* memory in the considered mechatronic system, and for testing the validity of the identified pre-sliding friction model. Fig. 8 compares the measured hysteresis friction loops with *nonlocal* memory (left column) with the simulated hysteresis loops (right column) showing a good agreement.

4. Breakaway force identification

Considering the typical hysteresis loop measurement corresponding to cylinder pressure variation with respect to supply pressure of 7-bar level, see Figs. 3 and 6, it is clear from the figures that the force tends to saturate with increasing displace-

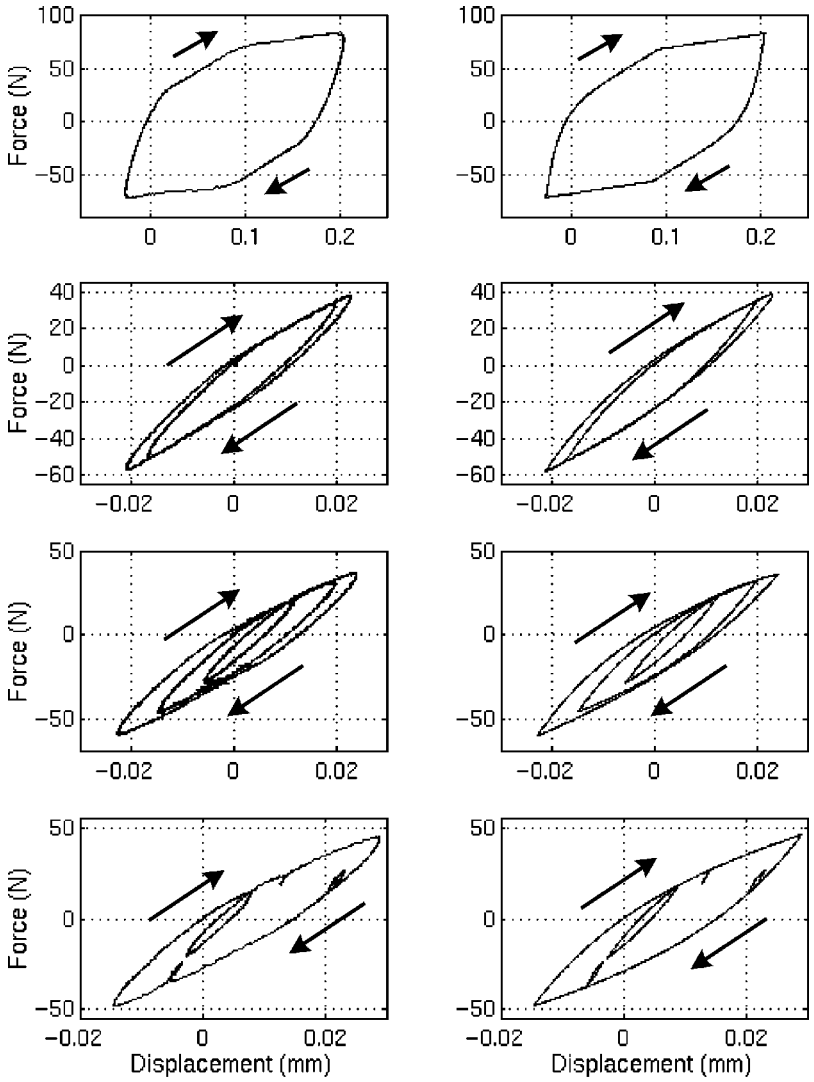

Fig. 8. Measured (left column) and simulated (right column) hysteresis friction loops with *nonlocal* memory.

ment. As a matter of fact, just after saturation, gross sliding will suddenly ensue. The value of the saturation force corresponds to the value of what is usually termed ''static friction'' or ''breakaway force.'' The displacement corresponding to the start of gross slip is termed ''pre-sliding distance.''

The breakaway experiments consist of ramping up the applied force that is proportional to the measured pressure difference in the chambers of the pneumatic cylinder until gross sliding occurs, and measuring synchronously the acceleration of the slider, the displacement and the force. The experimental results show that the measured acceleration is about zero within the pre-sliding regime then it suddenly increases from its zero point at the moment of break-away; see Fig. 9. When the synchronized data sets, pre-sliding displacement and force are plotted against each other, the pre-sliding distance and the breakaway force can be deduced; see Fig. 10.

Evidently, the friction behavior of the piston depends on the contact characteristics of its seals with the walls of the cylinder. It is therefore reasonable to expect this behavior to vary with the

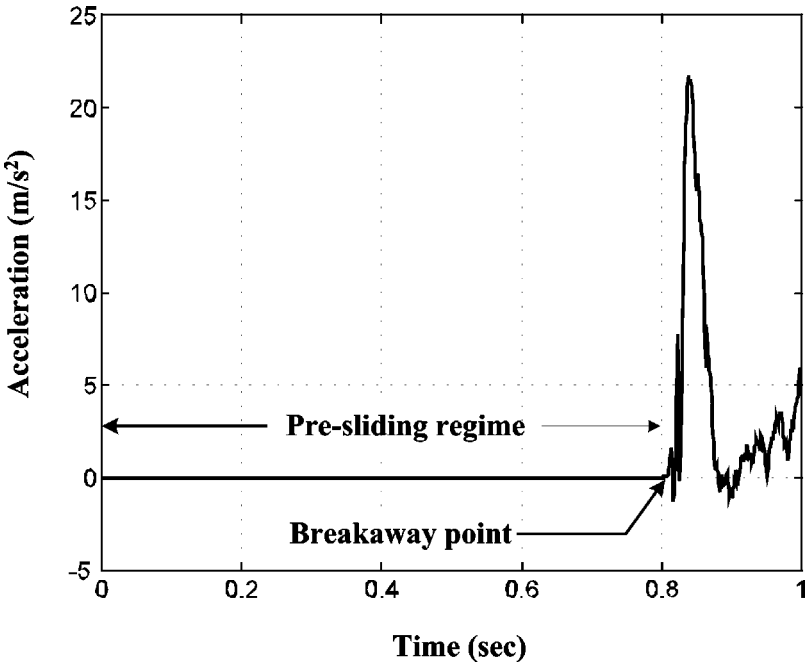

Fig. 9. Measured acceleration.

pressures on either side of the piston, since this will influence the contact force between the seals and the walls of the cylinder. Experiment has, in actual fact, confirmed this hypothesis. Since at the start of each friction test, the piston is at equilibrium with the pressures on either side both corresponding to the supply pressure (owing to inherent leakage of the valve), and that these pressures vary around that value during a test, a linear correlation has been found between the breakaway (or static) friction force (in both directions), and the supply pressure; see Fig. 11. The variation of the breakaway friction force with the gauge supply pressure is, however, small, being approximately 2.4 N/bar, or about 3% of the nominal value of the breakaway friction force per bar.

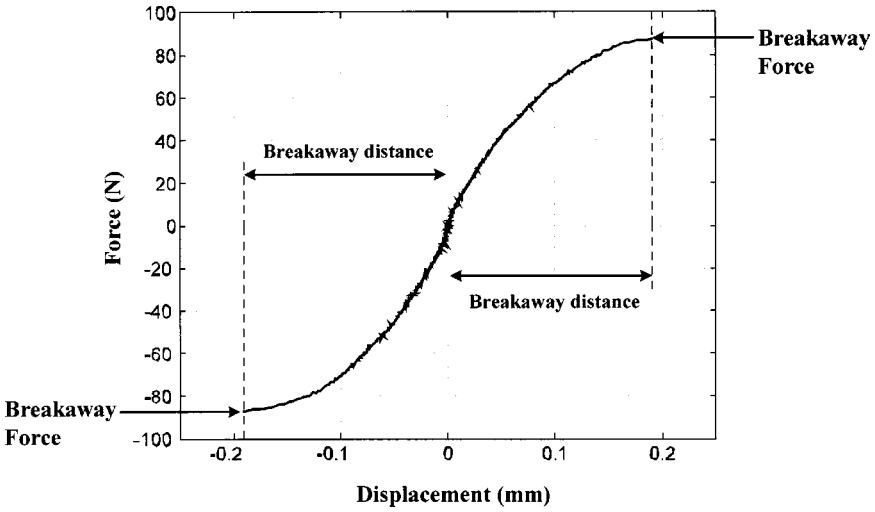

Fig. 10. Breakaway force and breakaway distance in the two directions.

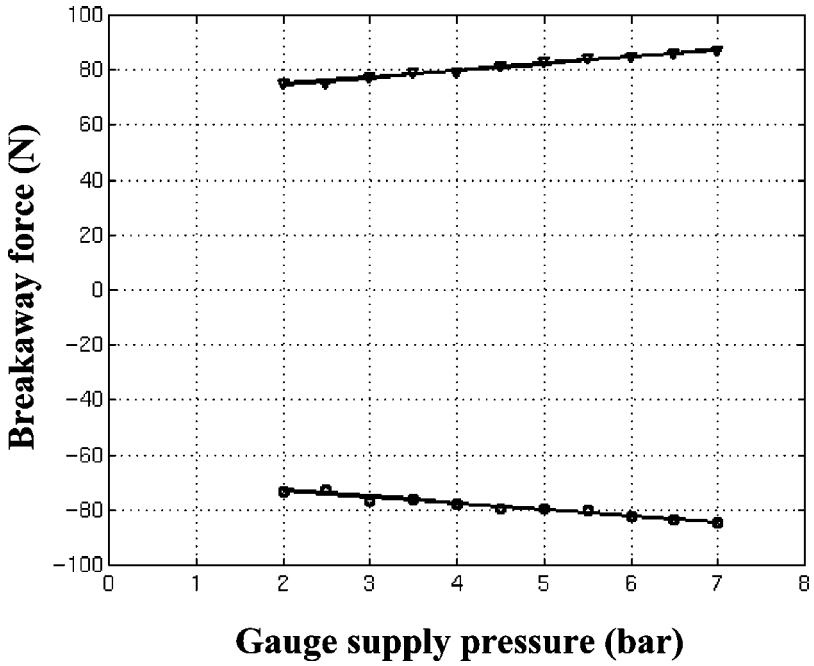

Fig. 11. Linear correlation between the breakaway (or static) friction force and the supply pressure.

5. Gross sliding friction identification

We now turn our attention to the identification of friction at gross sliding, i.e., the velocity dependence aspect. This is usually expressed in the form of Stribeck curve, which plots the friction force in function of the steady-state speed. In order to obtain this sort of data, however, the slide has to be run at a constant speed while the friction force is recorded, for a large number of speeds in the range of interest. Such a procedure is, however, almost impossible to execute on our system when it is pneumatically actuated, since it will require perfect control of the speed for which this investigation is a prerequisite. Instead, the line followed in this study is to excite the system so as to move periodically in the desired speed range, approximately $|\nu| \leqslant 2$ m/s, while recording the friction force. A series of tests have been carried out on the test setup, Fig. 1, for studying the velocity-dependent friction. In these experiments the velocity is calculated by integrating the measured acceleration and the friction force is calculated by multiplying the measured pressure difference between the two chambers of the cylinder with the cross-sectional area and subtracting the inertia force.

Typical results obtained with this procedure are depicted in Fig. 12, which plots the friction force in function of the velocity at different nominal chamber pressures corresponding to supply pressures of 2–7 bars (gauge), with steps of 1 bar. The results, which proved to be very repeatable, show quite clearly the hysteretic behavior of friction in the velocity or what is termed ''frictional lag'' (with respect to velocity change), see, e.g., Refs. [5–12]. That is to say that the friction force is higher for increasing speed (and lower for decreasing speed) than the quasistatic Stribeck value. The Stribeck behavior is very well in evidence, for the increasing speed part of the loop; it is characterized by an initial sharp fall in the friction force, reaching a minimum, and then a gradual increase that approaches a linear asymptote (corresponding to viscous friction). For decreasing speed, however, the behavior seems very consistently to resemble that of Coulomb plus viscous friction.

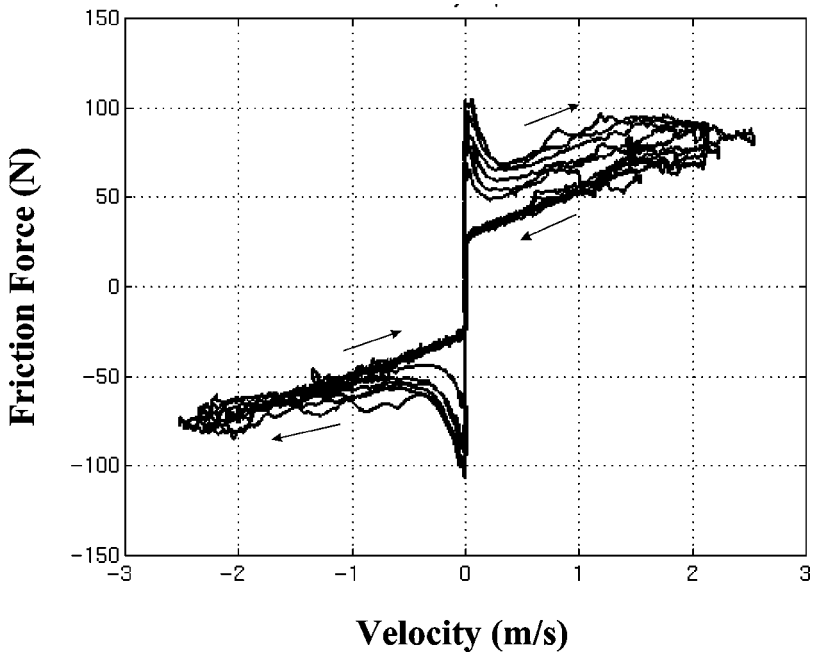

Fig. 12. Friction force in function of the velocity at different nominal chamber pressures corresponding to supply pressures of 2–7 bars (gauge), with steps of 1 bar.

In order to use the measured gross sliding friction in modeling, we fit the data separately for each branch of the hysteresis loop in function of the velocity such as shown in Fig. 13. A suitable gross sliding friction model would be

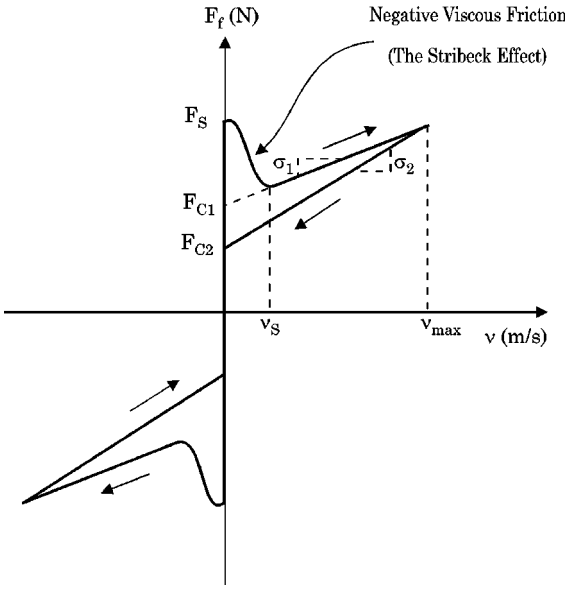

Fig. 13. Velocity-dependent friction model.

$$F_{\mathrm{f}}=\begin{cases}\operatorname{sgn}(\nu)F_{\mathrm{C1}}+\operatorname{sgn}(\nu)(F_{\mathrm{S}}-F_{\mathrm{C1}})\\ \quad\times\exp[(-|\nu|/\nu_{\mathrm{S}})^{\delta}]+\sigma_1\nu,\\ \quad\text{increasing speed}\\ \operatorname{sgn}(\nu)F_{\mathrm{C2}}+\sigma_2\nu,\ \text{decreasing speed},\end{cases}\tag{3}$$

where F_{f} is the friction force at gross sliding, $\operatorname{sgn}(\nu)$ is the sign of the velocity, ν is the velocity, F_{S} is the breakaway (or static) friction force, ν_{S} is the Stribeck velocity ($\nu_{\mathrm{S}}=0.2$ m/s), δ is the exponential parameter yielding the classical Stribeck effect ($\delta=2.5$), F_{C1} and F_{C2} are the Coulomb friction for increasing and decreasing speed, respectively, and $\sigma 1$ and $\sigma 2$ are viscous friction coefficients for increasing and decreasing speed, respectively.

6. Conclusions

An experimental method of friction identification with its two basic regimes, pre-sliding and gross sliding, is presented and demonstrated. The spring behavior of the asperity junctions of the contacting surfaces is verified by experiments. The *nonlocal* memory character of pre-sliding friction is verified by test. The pre-sliding friction is mod-

eled in function of stiffness and average deflection of the asperity junctions of the contacting surfaces. The gross sliding friction is identified and modeled in function of the velocity. The discontinuity between pre-sliding and gross sliding friction regimes is successfully eliminated by well modeling of the breakaway (or static) friction force, while the discontinuity between gross sliding and pre-sliding friction regimes (when the system goes from sliding to stiction) is eliminated by tracking the friction force during gross sliding, especially at the moment when the system goes from sliding to stiction.

For the purpose of solving the tracking (or the servo) problem of mechatronic systems, the experimentally identified and modeled friction in the considered mechatronic system can be used after updating some model parameters.

References

[1] Vo, H. P., NASA spins off better ball bearings. Mach. Des. February, 62–66 (1994).
[2] Prajogo, Tutuko, Experimental Study of Pre-rolling Friction for Motion-reversal Error Compensation on Machine Tool Drive Systems. Ph.D. thesis, Department of Mechanical Engineering, Division of Production Engineering, Machine Design and Automation (PMA), Katholieke Universiteit Leuven, Leuven, Belgium, 1999.
[3] Futami, S., Furutani, A., and Yoshida, S., Nanometer positioning and its micro-dynamics. Nanotechnology **1**, 31–37 (1990).
[4] Mayergoyz, I. D., Mathematical Models of Hysteresis. Springer Verlag, New York, 1991.
[5] Armstrong-Hèlouvry, B., Control of Machines with Friction. Kluwer Academic Publishers, London, 1991.
[6] Armstrong-Hèlouvry, B., Dupont, P., and De Wit, C. Canudas, A survey of models, analysis tools and compensation methods for the control of machines with friction. Automatica **30**, 1083–1138 (1994).
[7] De Wit, C. C., Olsson, H., Åström, and Lischinsky, A new model for control systems with friction. IEEE Trans. Autom. Control **40**, 419–425 (1995).
[8] Futami, S., Consideration of friction phenomena for precise position control. Jpn. J. Tribol. **38**, 1545–1552 (1993).
[9] Hess, D. P. and Soom, A., Friction at a lubricated line contact operating at oscillating sliding velocities. J. Tribol. **112**, 147–152 (1990).
[10] Nouri, Bashir M. Y., Al-Bender, F., Swevers, J., Vanherck, P., and Van Brussel, H., Identification, modeling and simulation of a pneumatic servo positioning system with friction. Proceedings of the IASTED International Conference: Modeling, Identification and Control, 2000, Innsbruck, Austria, pp. 421–427.
[11] Nouri, Bashir M. Y., Al-Bender, F., Swevers, J., Vanherck, P., and Van Brussel, H., Modeling a pneumatic servo positioning system with friction. Proceedings of American Control Conference, 2000, Chicago, Illinois, USA, pp. 1067–1071.
[12] Nouri, Bashir, Modeling and Control of Pneumatic Servo Positioning Systems. Ph.D. thesis, Department of Mechanical Engineering, Division of Production Engineering, Machine Design and Automation (PMA), Katholieke Universiteit Leuven, Leuven, Belgium, 2001.

Bashir M. Y. Nouri is Assistant Professor at the Department of Mechatronics Engineering at The Hashemite University. He received his Bachelor in Mechanical Engineering from Birzeit University, Palestine, in 1994, his Master in Water Resources Engineering from K. U. Leuven and V. U. Brussels, Belgium, in 1997, and his Ph.D. in Mechatronics from K. U. Leuven, Belgium, in 2001. His interests include identification, modeling, and simulation of mechatronic systems; control of industrial mechatronic systems, including robot control, classical control, and intelligent control; smart materials and smart structures; and transducers, interfacing, microcomputers, and data acquisitions systems. He is a member of the Jordanian Engineers Association.